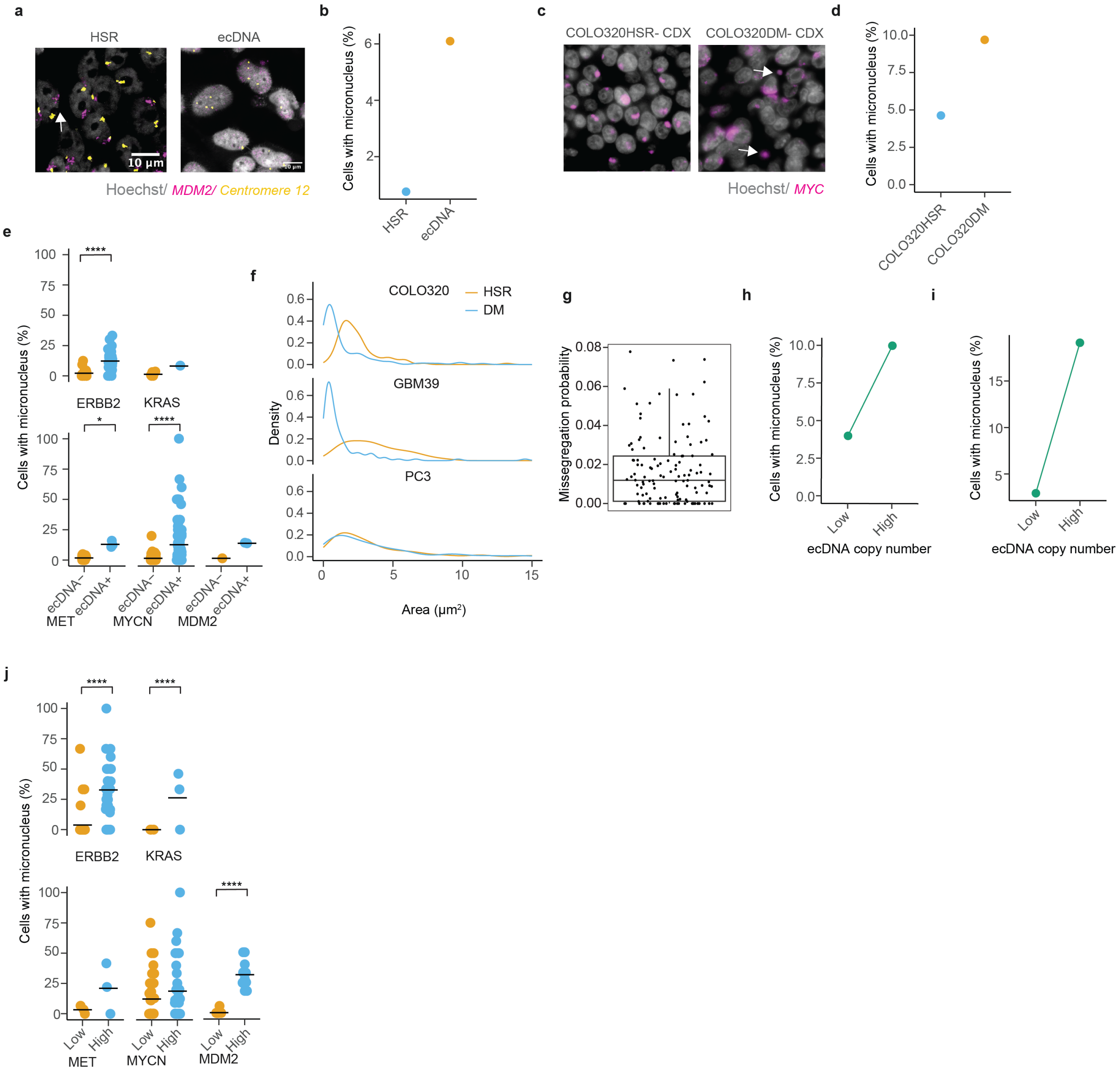

Extended Fig. 1: Cancer cells with high ecDNA content are prone to micronucleation irrespective of the amplified gene

a. Exemplary photomicrographs of *MDM2* amplified cell line models.

b. Fraction of cells with micronucleus in the *MDM2* amplified cell line model.

c. Exemplary photomicrographs of a CDX model of COLO320DM and COLO320HSR near isogenic cell line pair.

d. Fraction of cells with micronucleus in the CDX model.

e. Fraction of cells with micronucleus in patient tumor samples stratified by amplified gene (Student's t-test).

f. Density plot displaying micronuclei size distribution in three isogenic cell line pairs: COLO320DM (n=103), COLO320HSR (n=100), GBM39EC (n=100), GBM39HSR (n=33), PC3-DM (n=103) and PC3-HSR (n=102).

g. Mis-segregation probabilities across 8 cell lines and 119 patients.

h-j. Fraction of cells with micronuclei and low (bottom 30%) vs. high (top 30%) ecDNA content measured in the MDM2 amplified cell line model (h), the CDX model of COLO320DM and COLO320HSE (i), patient tumor samples stratified by amplified gene (j) (Student's t-test).

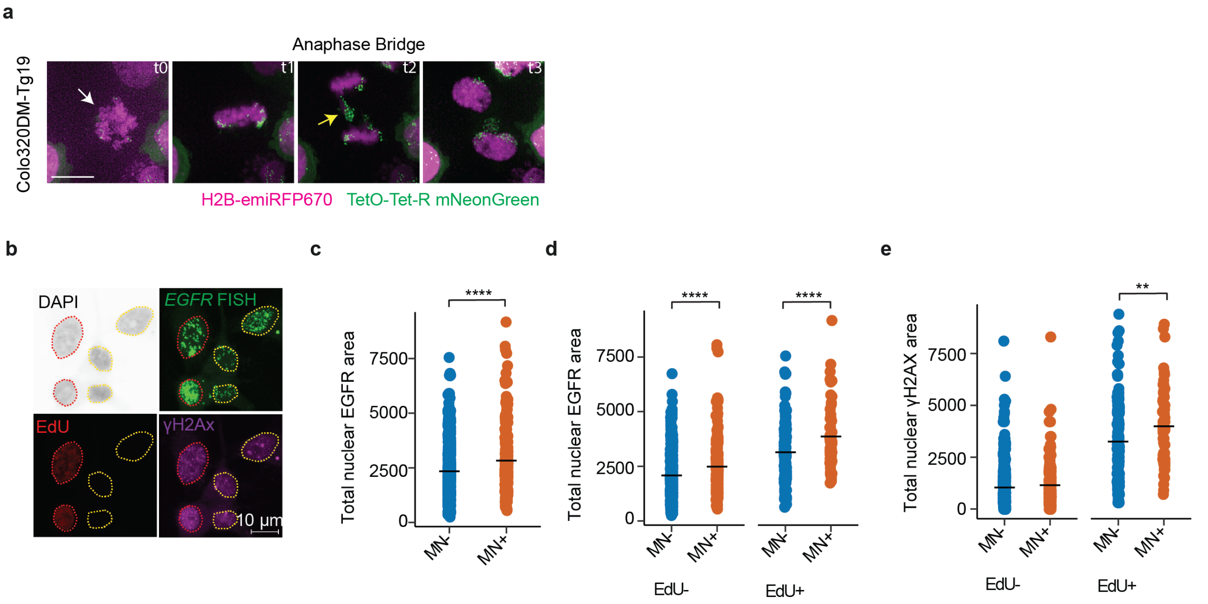

Extended Fig. 2: Higher micronucleation rate in high ecDNA copy number cells is not due to cell cycle arrest
a. Live-cell imaging of the COLO320DM-Tg19 cell line engineered to visualize MYC ecDNA (TetO-TetR-mNeonGreen) during mitotic transition. Representative snapshots of a mitotic cell (white arrow) undergoing mitosis with an anaphase bridge coated with ecDNA molecules (yellow arrow). Scale bar: 10µm.
b. Exemplary photomicrograph of EdU γH2Ax immunofluorescence and EGFR DNA FISH staining in GBM39ec cells. Red circled EdU+ S phase cells, and yellow circled EdU- non-S phase cells.
c. Total ecDNA content measured by DNA FISH staining in cells with or without micronuclei.
d. Total ecDNA content measured by DNA FISH staining in cells with or without micronuclei, with cell cycle stage inferred from EdU staining in primary nucleus: non-S phase: EdU-, S phase: EdU+.
e. DNA damage measure by γH2Ax staining in cells with or without micronuclei, with cell cycle stage inferred from EdU staining in primary nucleus: non-S phase: EdU-, S phase: EdU+.

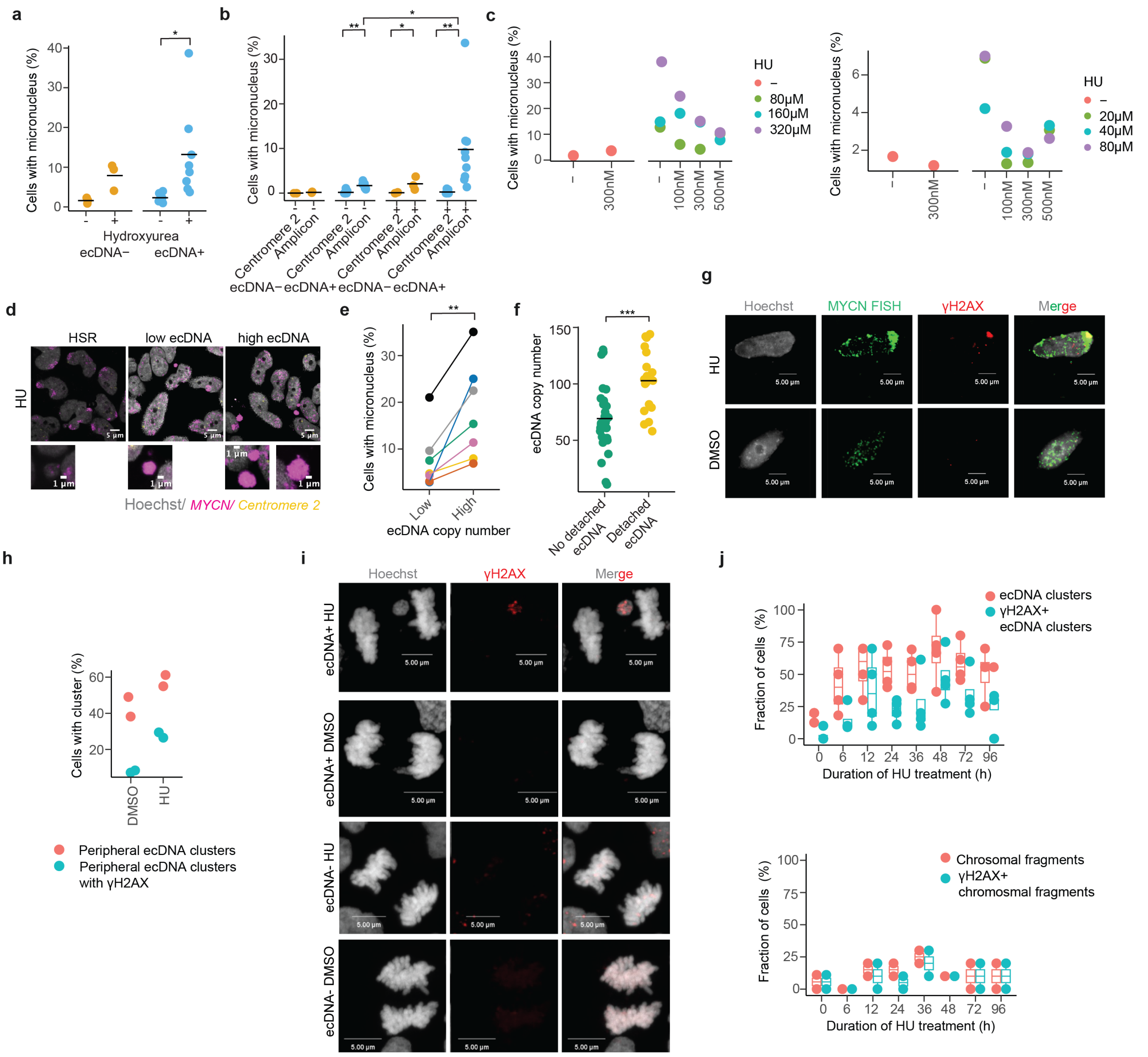

Extended Fig. 3: Induction of replication stress induces DNA damage, clustering in anaphase and micronucelation

a. Fraction of cells with micronuclei in cells with or without ecDNA in the presence or absence of hydroxyurea (80 µM) (One-way ANOVA).

b. Fraction of cells with micronuclei containing fluorescence signal after FISH for the amplicon or centromere 2 in cells with vs. without ecDNA (Two-way ANOVA).

c. Fractions of cells with micronucleus after parallel hydroxyurea treatment and dNTP supplementation for 3 days at different concentrations in two ecDNA cell lines.

d. Exemplary photomicrographs of cells with different ecDNA content and micronuclei (white arrowhead) in the presence of hydroxyurea (80 µM).

e. Fraction of cells with micronuclei at low (bottom 30%) vs. high (top 30%) ecDNA content after HU treatment (Paired Student's t-test).

f. Number of ecDNA copies per cell with attached or detached ecDNA clusters in anaphase after 80µM HU treatment for 24h (Student's t-test).

g. Exemplary photomicrographs of co-clustered ecDNA and immunofluorescent γH2AX foci in the nuclear periphery of interphase cells after 24 hours of hydroxyurea (80 µM) treatment and absence of co-clustering in DMSO treated cells.

h. Frequency of total ecDNA clusters and γH2AX-positive ecDNA clusters in the nuclear periphery of interphase cells after 24 hours of treatment with hydroxyurea (80 µM) vs. DMSO.

i. Exemplary photomicrographs of lagging ecDNA co-clustering with immunofluorescent γH2AX in anaphase cells after hydroxyurea (80 µM) treatment in ecDNA-positive cells and absence of lagging DNA in DMSO treated cells and in ecDNA-negative cells.

j. Frequency of total lagging ecDNA clusters and γH2AX-positive lagging ecDNA clusters in ecDNA-positive anaphase cells (top) and frequency of lagging chromosomal fragments in ecDNA-negative anaphase cells (bottom), across increasing durations of hydroxyurea (80 µM) treatment.

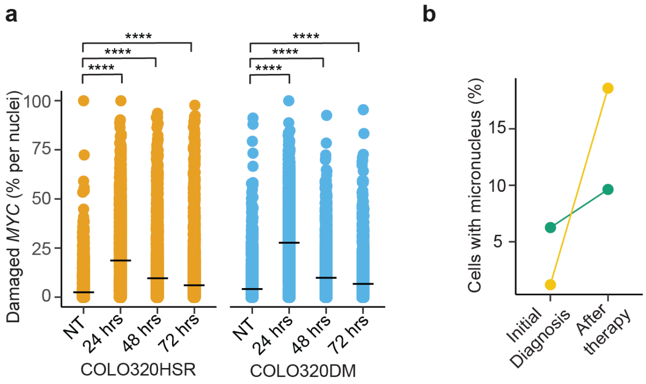

Extended Fig. 4: Nucleofection with Cas9 induces DNA induction at target site
a. Fraction of damaged *MYC* in *MYC* amplified near isogenic cell lines at different timepoints after nucleofection.
b. Fraction of cells with micronuclei in two patient pairs before and after standard of care chemotherapy.

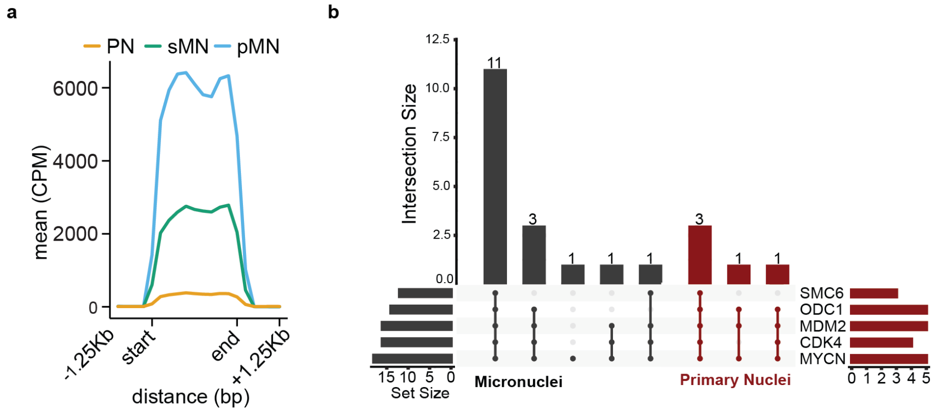

Extended Fig. 5: EcDNA mis-segregates into micronuclei en masse.

a. Signal plot of the mean coverage over length-scaled ecDNA regions in single primary nuclei (PN, n = 5), single micronuclei (sMN, n = 19) and pooled micronuclei (pMN, n = 7).

b. UpSet plot of co-occurrence of 5 ecDNA species in single micronuclei and primary nuclei.

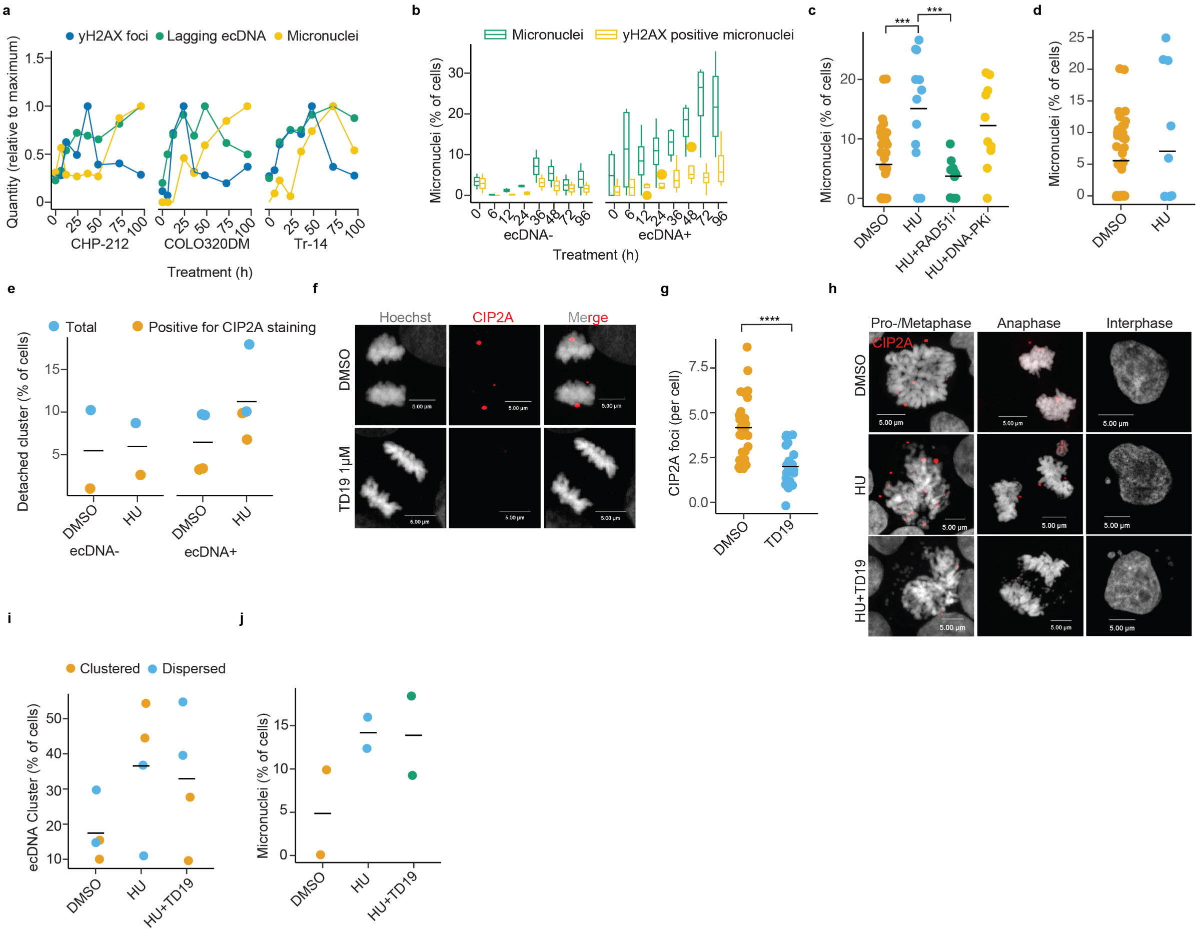

Extended Fig. 6: Replication stress-induced DNA damage in interphase is associated with detachment of ecDNA during mitosis and can be alterated by chemical inhibition

a. Quantity of γH2AX foci, lagging ecDNA and micronuclei as fractions of their respective maxima across increasing durations of hydroxyurea (80 µM) treatment in three ecDNA-positive cell lines.

b. Frequency of total micronuclei and γH2AX-positive micronuclei in two ecDNA-negative and four ecDNA-positive cell lines across increasing durations of hydroxyurea (80 µM) treatment.

c. Fraction of cells with micronucleus in COLO320DM cell line treated with HU in addition to a RAD51 or DNA-PK inhibitor (One-way ANOVA).

d. Fraction of cells with micronucleus in COLO320HSR cell line treated with HU.

e. Frequency of total lagging DNA and lagging DNA staining positive for CIP2A during anaphase after 24 hours of DMSO or hydroxyurea (80 µM).

f. Exemplary photomicrographs of a cell with ecDNA in anaphase stained using immunofluorescence against CIP2A (red) in untreated cells and in cells treated with 1µM TD-19.

g. Quantification of CIP2A foci in anaphase in untreated cells and in cells treated with 1µM TD-19 (Student's t-test).

h. Exemplary photomicrographs of CIP2A immunofluorescence staining during pro-/metaphase and interphase after 24 hours of DMSO, hydroxyurea (80 µM) or hydroxyurea (80 µM) and TD-19 (1 µM).

i. Frequency of clustered lagging ecDNA and dispersed lagging ecDNA during anaphase in two ecDNA-positive cell lines after 24 hours of DMSO, hydroxyurea (80 µM) or hydroxyurea (80 µM) and TD-19 (1 µM).

j. Frequency of micronuclei in two ecDNA-positive cell lines after 24 hours of DMSO, hydroxyurea (80 µM) or hydroxyurea (80 µM) and TD-19 (1 µM).

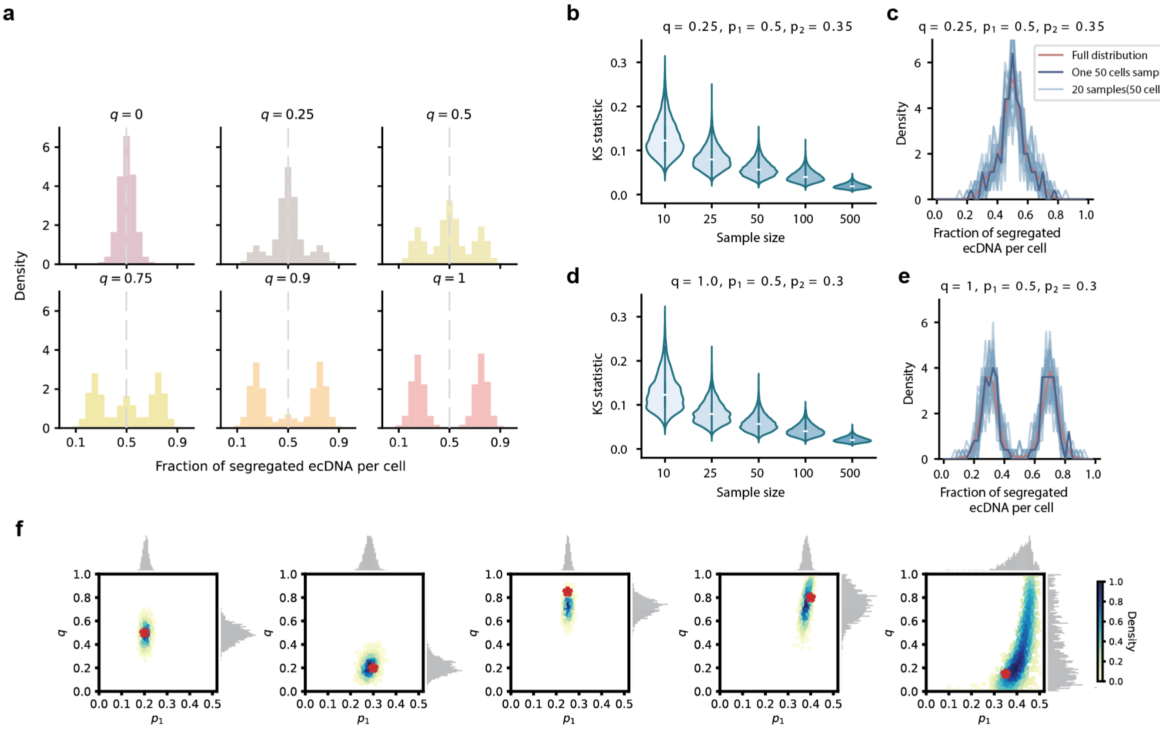

Extended Fig. 7: A biased random-segregation model.

a. Simulated distributions of ecDNA fractions under varying q values (proportion of biased segregation), with $p_1 = 0.25$ (extent of biased segregation).

b-e. Comparison of ecDNA fraction distributions under different sample sizes. (b) Violin plot showing the Kolmogorov distances between the sampled distributions and the full distribution across varying sample sizes. (c) Comparison of ecDNA fraction distributions: the red line represents the full distribution generated from 10^7 cell divisions, while the blue line represents the distribution based on 50 sampled ecDNA fractions.

d-e. Same analyses as shown in (b) but generated using different parameters as indicated in the figure. f. Density scatter plot of inferred parameters p_1 and q using synthetic data (50 pairs of daughter cells) for different combinations p_1 and q. The marginal distributions of p_1 and q are displayed above and to the right, respectively. Density values are normalized to 1. The red star indicates the true parameter values.

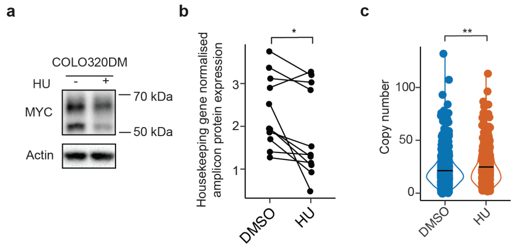

Extended Fig. 8: Short term HU treatment increases ecDNA copy number but reduces protein expression

a. MYC expression as measured using western immunoblotting of cells with or without ecDNA in the presence or absence of hydroxyurea (80 µM).

b. Housekeeping gene normalized MYC protein expression in cells incubated with hydroxyurea (80 µM) or DMSO (vehicle control).

c. Oncogene copy numbers as measured using FISH in COLO320DM cells after 3d of HU treatment (Student’s t-test).

a

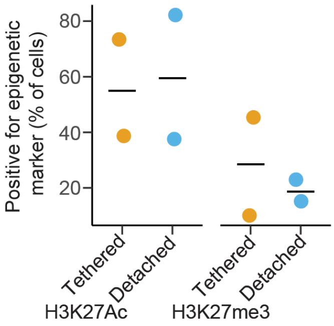

Extended Fig. 9: Detachment of ecDNA during mitosis does not affect chromatin modifications on ecDNA.
a. Frequency of tethered vs. detached ecDNA during anaphase with positive immunofluorescent staining for H3K27Ac or H3K27Me3 in two cell lines with ecDNA.

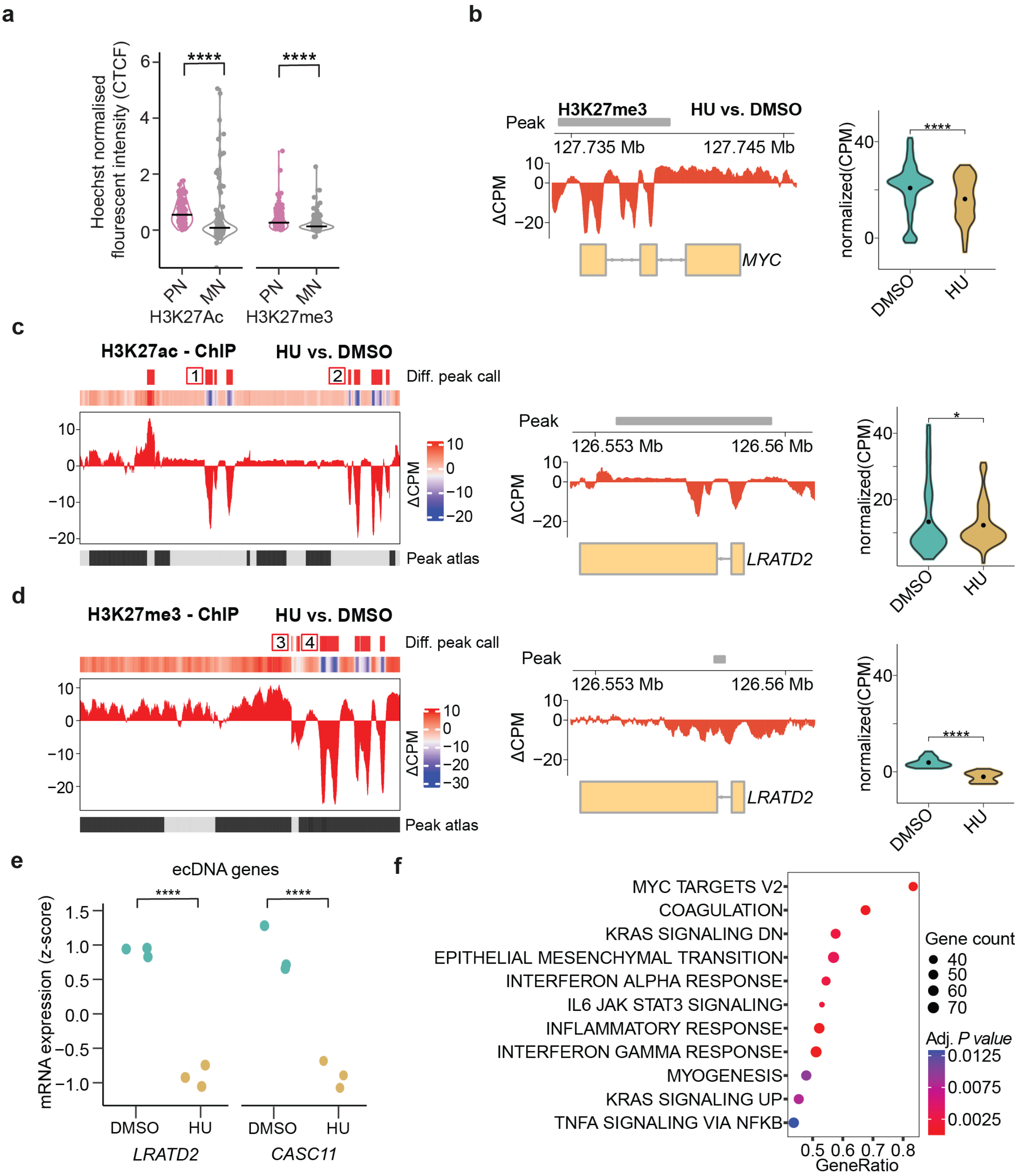

Extended Fig. 10: Inducing micronucleation of ecDNA promotes epigenetic remodelling and transcriptional repression of oncogenes.

a. Hoechst normalized H3K27Ac and H3K27me3 intensity in micronuclei vs. primary nuclei in COLO320DM cells (One-way ANOVA).

b. ChIP-sequencing of H3K27me3 in COLO320DM cells. Left panel: from top to bottom: peak call annotation. DMSO-subtracted read density as counts per million (CPM). Gene annotation. Right panel: Input-subtracted read density as CPM.

c-d. Epigenetic profiles of HU and DMSO-treated cells, (c) H3K27Ac and (d) H3K27me3. Left panel: from top to bottom: Regions with distinct change in read density (Methods); numbers depict peak regions containing genes. DMSO-substracted read density as counts per million (CPM). Merged peak atlas regions (Methods). Middle panel: from top to bottom: Peak call annotation. DMSO-subtracted read density as counts per million (CPM). Gene annotation. Right panel: Input-normalized read density as CPM.

e. Z-score normalized transcript count of genes amplified on ecDNA. 3 replicates per treatment condition. Benjamini-Hochberg procedure-corrected p-values are shown (Wald test).

f. Significantly enriched MSigDBhallmark genesets between hydroxyurea and DMSO treated cells. Benjamini-Hochberg procedure-corrected p-values andgene counts are shown.